

Avoided-crossing-based liquid-crystal photonic-bandgap notch filter

Danny Noordegraaf,^{1,*} Lara Scolari,¹ Jesper Lægsgaard,¹ Thomas Tangaard Alkeskjold,¹ Giovanni Tartarini,² Elena Borelli,² Paolo Bassi,² Jun Li,³ and Shin-Tson Wu³

¹COM-DTU Department of Communications, Optics and Materials, Technical University of Denmark, DK-2800, Denmark

²Dipartimento di Elettronica Informatica e Sistemistica, University of Bologna, Viale Risorgimento, 2 I 40136 Bologna, Italy

³College of Optics and Photonics, University of Central Florida, Orlando, Florida 32816, USA

*Corresponding author: dno@com.dtu.dk

Received October 18, 2007; revised February 21, 2008; accepted February 24, 2008; posted March 21, 2008 (Doc. ID 88710); published April 29, 2008

We demonstrate a highly tunable deep notch filter realized in a liquid-crystal photonic-bandgap (LCPBG) fiber. The filter is realized without inducing a long-period grating in the fiber but simply by filling a solid-core photonic-crystal fiber with a liquid crystal and exploiting avoided crossings within the bandgap of the LCPBG fiber. The filter is demonstrated experimentally and investigated using numerical simulations. A high degree of tuning of the spectral position of the deep notch is also demonstrated. © 2008 Optical Society of America

OCIS codes: 060.2310, 230.3990, 230.3720, 230.7408.

Photonic-crystal fibers (PCFs) are a special kind of light-guiding fibers consisting of a cladding structure of air holes running along the length of the fiber. Such a structure allows for the infiltration of various materials into the cladding, making it possible to create highly tunable fiber devices [1].

By filling a PCF with a material having a higher refractive index than silica, a photonic-bandgap (PBG) fiber is created. Such a fiber guides owing to multiple reflections from the high-index material and silica interfaces and will transmit light in a number of wavelength intervals [2,3]. When a liquid crystal (LC) is infiltrated into the air-hole structure of a PCF, tunable fiber devices can be realized where the transmission properties of the fiber can be tuned by changing temperature or applying an electric field [4–7].

Recently, deep notch filters have been realized in PBG fibers by inducing a mechanical long-period grating in the fiber [8]. Such a grating results in a coupling of the fundamental core mode to higher-order modes (HOMs) of the fiber core or cladding. These HOMs have a high loss, and deep notches in the transmission windows of the fiber are realized. Furthermore, both mechanical and electrically induced LPGs have been induced in liquid-crystal photonic-bandgap (LCPBG) fibers [9].

In this Letter, deep notch filters in PBG fibers are demonstrated without using gratings but simply by exploiting the properties of the material and the fiber to create a loss in a narrow wavelength band. The fiber used in the experiment is a silica large-mode-area (LMA-10) fiber from Crystal Fibre A/S. The diameter of the holes is $3.45\ \mu\text{m}$, the interhole distance is $7.15\ \mu\text{m}$, and the diameter of the core is $\sim 10\ \mu\text{m}$. Figure 1(a) shows a scanning electron microscope (SEM) image of the fiber end facet.

The LC used is MDA-00-3969, fabricated by Merck (Germany). It has ordinary and extraordinary indices

of $n_o = 1.4929$ and $n_e = 1.6986$, respectively, at a wavelength of $656\ \text{nm}$ and at a temperature of 30°C . The alignment of the LC inside the capillary tubes of the fiber cladding is investigated by using polarization microscopy on a single capillary tube filled with the LC. The LC inside a capillary tube has a splayed alignment. In the center, the LC is aligned parallel to the capillary and, at the surface, the LC has an angle of 45° with the capillary wall [6]. The alignment is illustrated in Fig. 1(b).

The LC is infiltrated 20 mm into the fiber. Filling is done at room temperature and purely by using capillary forces. The transmission of the LCPBG fiber is measured using the setup shown in Fig. 1(c). Light from a tungsten-halogen white-light source is coupled into the LCPBG fiber device using an un-

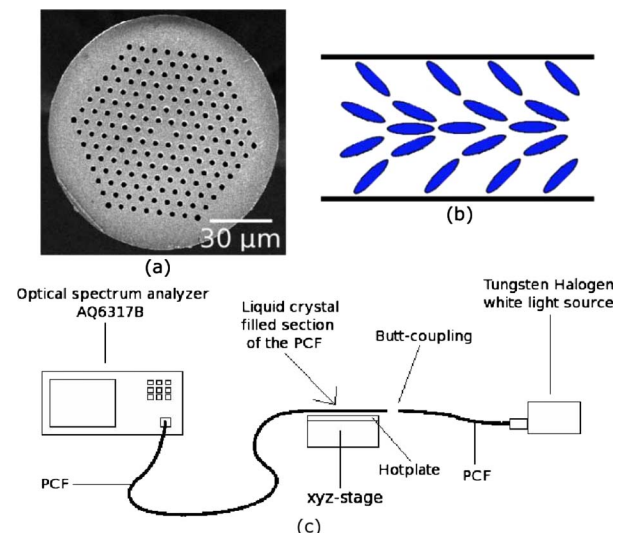


Fig. 1. (Color online) (a) SEM image of PCF end facet. (b) Splay alignment of the LC. (c) Setup used to measure the transmission of the LCPBG fiber.

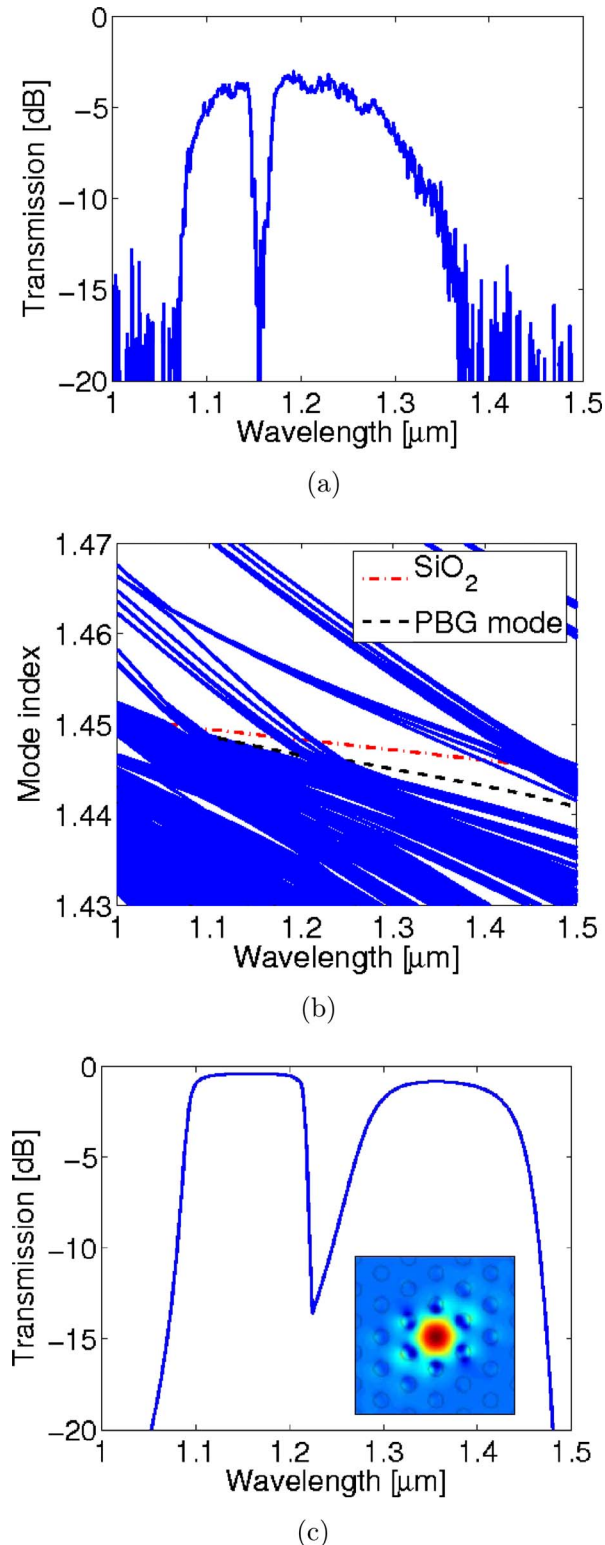


Fig. 2. (Color online) Measured and simulated results at a temperature of 30°C. (a) Measured transmission spectrum of the LC-filled fiber. (b) Simulated effective mode indices of modes in the high-index LC-filled rods (solid curves) and the core-guided mode (dashed curve). The avoided crossing of the core mode is shown in the center of the transmission band. (c) Simulated transmission spectrum of the LC-filled fiber. Both coupling and propagation loss are taken into account. Inset shows the dominant x component of the electric field of the fundamental core mode at a wavelength of 1.35 μm .

filled PCF. The two fibers are aligned on an xyz stage, and the transmission is measured using an optical spectrum analyzer. Figure 2(a) shows the transmission spectrum of the LCPBG fiber, normalized to that of an unfilled fiber. The spectrum shows a notch in the transmission at a wavelength of 1160 nm in the bandgap from ~ 1070 to ~ 1360 nm. The 3 dB width of the notch is 21 nm. This notch in the transmission spectrum is caused by a cladding mode with a cutoff at this wavelength. The fiber cladding therefore becomes transparent at this wavelength, and light cannot be confined in the fiber core. Numerical simulations of the mode indices of the high-index LC filled rods have been made using a plane-wave expansion method [10]. The simulations take the splayed alignment of the LCs into account. The result is shown in Fig. 2(b), represented by the solid curves. The effective index of the fundamental core-guided mode is also calculated and is shown with a dashed curve. In Fig. 2(b) two bandgaps can be seen, one centered at a wavelength of ~ 1150 nm and one at ~ 1350 nm. Compared to the measured transmission, the bandgap edges are shifted toward longer wavelengths in the simulations. The short and the long wavelength edge of the left bandgap and the short wavelength edge of the right bandgap are shifted ~ 50 nm toward longer wavelengths. We believe that the reason for this shift is that the refractive indices of the LC used in the simulations are measured at visible wavelengths and then extrapolated to the infrared. A large shift of the measured and simulated long wavelength edge of the right bandgap is, however, observed where the simulations indicate that the bandgap should extend to a wavelength of ~ 1500 nm. The reason that the measured transmission does not extend this far is probably due to a large coupling of the core mode to the cladding in the long wavelength region of the bandgap. The cladding mode that creates the notch in the transmission has been found to be a LP_{31} -type mode. A more detailed investigation of the types of modes that create the bandgaps will follow in a future publication.

To further understand the physical nature of the notch, simulations of the coupling and propagation loss of the fundamental core guided mode have also been made. This was done using a finite-element solver, capable of taking into account the anisotropic LC rods in the cladding of the PCF [11,12]. The total calculated loss is shown in Fig. 2(c) and does indeed show the same notch in the transmission spectrum, as observed in the measured transmission. As for the plane-wave calculations, a slight shift of ~ 50 nm of the bandgap edges is observed here as well. Furthermore, the simulations show a smaller loss in the bandgaps (<1 dB) than what is measured (~ 4 dB). The shape of the calculated transmission is also slightly different. While the short wavelength edge of the left bandgap in the simulations is very sharp, it is more smoothed in the measured spectrum. For the short wavelength edge of the right bandgap, the opposite is true, i.e., it is smooth in the simulations but very sharp in the measured spectrum. Finally, the 3 dB width of the simulated notch is 62 nm, which is

three times more than the measured width. The reasons for these differences are, as for the plane-wave calculations, that there is an uncertainty in the refractive indices and in the average hole size that is used in the simulations. Furthermore, both size variations between different holes and scattering/absorption of light have been neglected in the calculations, which will result in a general loss, especially at the bandgap edges. In spite of these differences between the calculated and the measured spectrum, the finite-element calculations provide an excellent method to predict the approximate transmission spectrum.

By changing the temperature of the LC, the spectral position of the loss dip can be tuned. Figure 3(a) shows the transmission of the LCPBG fiber at temperatures of 30°C and 65°C. When the temperature is increased the loss dip moves towards shorter wavelengths. Figure 3(b) shows the spectral position of the loss dip as a function of temperature. A linear fit of the measured spectral position shows that a tuning

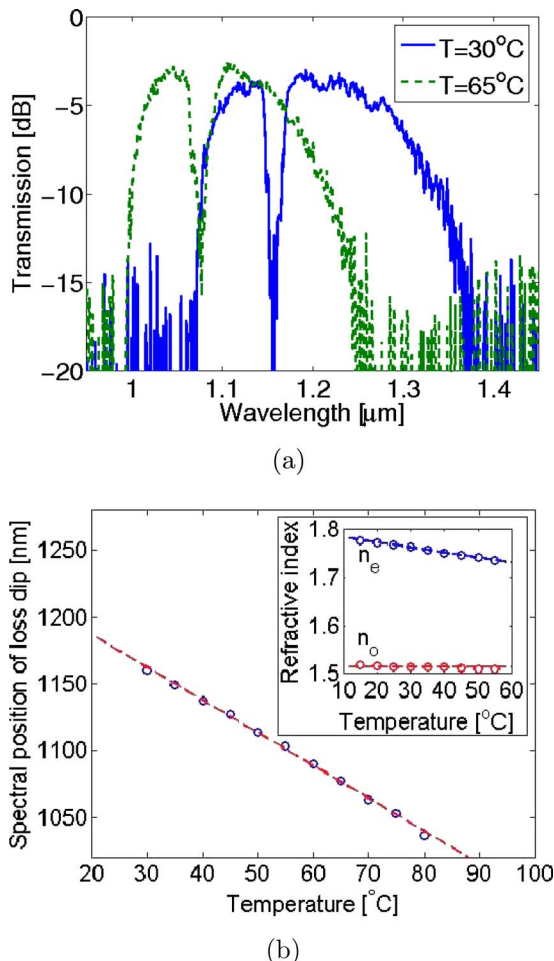


Fig. 3. (Color online) (a) Transmission spectrum of the LC filled fiber at temperatures of 30°C and 65°C. (b) Spectral position of the loss dip as a function of temperature. A tuning of $-2.5 \text{ nm}/^\circ\text{C}$ is achieved over 124 nm. Inset, n_o and n_e of the LC MDA-00-3969, as a function of temperature, at a wavelength of 450 nm. The clearing point of the LC is 106°C.

of $-2.5 \text{ nm}/^\circ\text{C}$ is achieved. The shift can be explained by the refractive indices of the LC as a function of temperature, shown in the inset of Fig. 3(b). Here the ordinary index of the LC is almost constant, whereas the extraordinary index decreases linearly at temperatures well below the clearing point [13]. This results in the linear tuning of the notch.

In conclusion, we have demonstrated a simple method of realizing a deep notch filter by exploiting the properties of a LC and a PCF. The filter can be tuned by temperature, and a tuning of $-2.5 \text{ nm}/^\circ\text{C}$ over 124 nm is demonstrated. The characteristics of the notch filter have been modeled using both a plane-wave and a finite-element method. The first method was used to calculate the position of the bandgaps, and the second was used to estimate the transmission spectrum by calculating the coupling and propagation loss of the LC device. The simulations are in agreement with the measured transmission spectrum, except for a shift of $\sim 50 \text{ nm}$, caused by small structural variations of the fiber and the fact that there is some uncertainty in determining the refractive indices of the LC. If the diameter of the holes of the PCF is increased, the bandgaps will move towards longer wavelengths. By carefully tailoring the parameters of the fiber it will therefore be possible to move the deep notch to telecom wavelengths, thereby realizing a simple optical component that can be easily integrated into an optical communication link.

References

1. B. J. Eggleton, C. Kerbage, P. S. Westbrook, R. S. Windeler, and A. Hale, *Opt. Express* **9**, 698 (2001).
2. N. M. Litchinitser, S. C. Dunn, P. E. Steinvurzel, B. J. Eggleton, T. P. White, R. C. McPhedran, and C. M. de Sterke, *Opt. Express* **12**, 1540 (2005).
3. R. T. Bise, R. S. Windeler, K. S. Kranz, C. Kerbage, B. J. Eggleton, and D. J. Trevor, in *Optical Fiber Communication Conference* (Optical Society of America, 2002), paper ThK3.
4. T. T. Larsen, A. Bjarklev, D. S. Hermann, and J. Broeng, *Opt. Express* **11**, 2589 (2003).
5. F. Du, Y. Q. Lu, and S. T. Wu, *Appl. Phys. Lett.* **85**, 2181 (2004).
6. L. Scolari, T. T. Alkeskjold, J. Riishede, A. Bjarklev, D. S. Hermann, A. Anawati, M. D. Nielsen, and P. Bassi, *Opt. Express* **13**, 7483 (2005).
7. T. R. Wolinski, K. Szaniawska, S. Ertman, P. Lesiak, A. W. Domanski, R. Dabrowski, E. N. Kruszelnicki, and J. Wojcik, *Meas. Sci. Technol.* **17**, 985 (2006).
8. P. Steinvurzel, E. D. Moore, E. C. Magi, B. T. Kuhlmeier, and B. J. Eggleton, *Opt. Express* **14**, 3007 (2006).
9. D. Noordegraaf, L. Scolari, J. Lægsgaard, L. Rindorf, and T. T. Alkeskjold, *Opt. Express* **15**, 7901 (2007).
10. S. G. Johnson and J. D. Joannopoulos, *Opt. Express* **8**, 173 (2001).
11. G. Tartarini, M. Pansera, T. T. Alkeskjold, A. Bjarklev, and P. Bassi, *J. Lightwave Technol.* **25**, 2522 (2007).
12. G. Tartarini, R. Stolte, and H. Renner, *Opt. Commun.* **253**, 109 (2005).
13. J. Li, S. Gauza, and S. T. Wu, *Appl. Phys. Lett.* **96**, 19 (2004).